

Structure Determination of Two Modulated γ -Brass Structures in the Zn–Pd System through a (3 + 1)-Dimensional Space Description

Olivier Gourdon,^{*,†} Zunbeltz Izaola,[‡] Luis Elcoro,[§] Vaclav Petricek,^{||} and Gordon J. Miller[⊥]

[†]Jülich Center for Neutron Science—Neutron Scattering Science Division, Oak Ridge National Laboratory, Oak Ridge, Tennessee 37831-6032, [‡]Helmholtz Zentrum Berlin, Glienicker Strasse 100, D-14109 Berlin, Germany, [§]F. Ciencia y Tecnología, Dept. Fis. Mat. Condensada, Univ. Pais Vasco, Apdo 644, E-48080 Bilbao, Spain, ^{||}Institute of Physics, Academy of Sciences of the Czech Republic, Na Slovance 2, 180 40 Praha 8, Czech Republic, and [⊥]Department of Chemistry and Ames Laboratory, U.S. Department of Energy, Iowa State University, Ames, Iowa 50011-3111

Received May 1, 2009

The structure determination of two composite compounds in the Zn–Pd system with close relationships to the cubic γ -brass structure $\text{Zn}_{11-\delta}\text{Pd}_{2+\delta}$ is reported. Their structures have been solved from single crystal X-ray diffraction data within a (3 + 1)-dimensional [(3 + 1)D] formalism. $\text{Zn}_{75.7(7)}\text{Pd}_{24.3}$ and $\text{Zn}_{78.8(7)}\text{Pd}_{21.2}$ crystallize with orthorhombic symmetry, superspace group $Xmmm(00\gamma)0s0$ ($X = [(1/2, 1/2, 0, 0); (0, 1/2, 1/2, 1/2); (1/2, 0, 1/2, 1/2)]$), with the following lattice parameters, respectively: $a_s = 12.929(3)$ Å, $b_s = 9.112(4)$ Å, $c_s = 2.5631(7)$ Å, $q = 8/13 c^*$ and $V_s = 302.1(3)$ Å³ and $a_s = 12.909(3)$ Å, $b_s = 9.115(3)$ Å, $c_s = 2.6052(6)$ Å, $q = 11/18 c^*$ and $V_s = 306.4(2)$ Å³. Their structures may be considered as commensurate because they can be refined in the conventional 3D space groups (*Cmce* and *Cmcm*, respectively) using supercells, but they also refined within the (3 + 1)D formalism to residual factors $R = 3.14\%$ for 139 parameters and 1184 independent reflections for $\text{Zn}_{75.7(7)}\text{Pd}_{24.3}$ and $R = 3.16\%$ for 175 parameters and 1804 independent reflections for $\text{Zn}_{78.8(7)}\text{Pd}_{21.2}$. The use of the (3 + 1)D formalism improves the results of the refinement and leads to a better understanding of the complexity of the atomic arrangement through the various modulations (occupation waves and displacive waves). Our refinements emphasize a unique Pd/Zn occupancy modulation at the center of distorted icosahedra, a modulation which correlates with the distortion of these polyhedra.

Introduction

Our exploration of new aperiodic compounds in the Zn-rich portion of the Zn–Pd system has been motivated by the idea that a prototype 1D quasicrystal, as defined by the Fibonacci sequence, can be regarded both as a quasicrystal and as an incommensurately modulated crystal.¹ Consequently, there are two different ways to achieve such atomic structures. In the Zn–Pd system we have demonstrated, using single crystal X-ray diffraction, that the γ -brass phase identified for 75.7(7)–81.9(6) atomic percent Zn is one member of a family of intergrowth compounds.^{2,3} These compounds change from one to the other by their chemical composition as well as the way the Pd-centered polyhedra, that is, icosahedra and distorted icosahedra, are connected together. Similar behavior has been observed in the Zn–Ni

and Zn–Pt systems as well.^{4,5} At present, we have been able to isolate six different Zn–Pd structures based on the cell parameters refined by single crystal X-ray diffraction.^{2,3} Among these six structures, two compounds formulated as $\text{Zn}_{81.9(6)}\text{Pd}_{18.1}$ and $\text{Zn}_{75.7(7)}\text{Pd}_{24.3}$ have been fully refined regarding the atomic positions and site occupancies in the conventional space groups, $\bar{I}43m$ and *Cmce*, respectively. The cubic $\text{Zn}_{81.9(6)}\text{Pd}_{18.1}$ phase adopts the Hume–Rothery γ -brass structure with 52 atoms per unit cell and an alternative formulation of $\text{Zn}_{10.65(1)}\text{Pd}_{2.35}$. Since $\text{Zn}_{81.9(6)}\text{Pd}_{18.1}$ and $\text{Zn}_{75.7(7)}\text{Pd}_{24.3}$ correspond to the limiting compositions of the “ γ -brass region” of the Zn–Pd phase diagram but show distinctly different crystal structures,² they are considered to be “parent compounds” in a Farey tree description of possible intergrowth structures,^{5,6} with commensurate

*To whom correspondence should be addressed. E-mail: gourdonoa@ornl.gov.

(1) Lifshitz, R. *Found. Phys.* **2003**, *33*, 1703.

(2) Gourdon, O.; Miller, G. J. *Chem. Mater.* **2006**, *18*, 1848.

(3) Gourdon, O.; Izaola, Z.; Elcoro, L.; Petricek, V.; Miller, G. J. *Philos. Mag.* **2006**, *86*(3–5), 419.

(4) Schmidt, J. D.; Lee, S.; Fredrickson, D. C.; Conrad, M.; Sun, J.; Harbrecht, B. *Chem.—Eur. J.* **2007**, *13*, 1394.

(5) Thimmaiah, S.; Richter, K. W.; Lee, S.; Harbrecht, B. *Solid State Sci.* **2003**, *5*, 1309.

(6) The Farey Series of Order 1025. In *Royal Society Mathematical Tables*; Cambridge University Press: Cambridge, 1950; Vol. I.

modulations 3/5 and 8/13, respectively. This behavior differs from the γ -brass region of the Cu–Zn diagram, which also exhibits a phase width between 57 and 68 atomic percent Zn.^{7,8} These parent structures could be refined using standard treatments because their periodicity is sufficiently short to perform such a strategy. The problem encountered for the other four structures, where the sizes of their unit cells do not allow this treatment, demand them to be considered as misfit structures and so to consider a refinement using (3 + 1)D superspace groups.^{9–11}

The aim of this work is to determine a refinement model of these intermediate structures using (3 + 1)D superspace groups, which may allow us to refine any intergrowth structures in this Zn-rich region of the Zn–Pd system that we may be able to synthesize. To develop this model, we have utilized $\text{Zn}_{75.7(7)}\text{Pd}_{24.3}$ because it has already been refined by the standard treatment and, thus, can be easily compared by both refinement strategies. Moreover, the ratio of the periodicities along a particular unit cell direction, identified as 8/13, is sufficiently large to avoid possible errors or missing information on the nature of the modulations. In addition to refinement of this 8/13 modulated phase, we present the refinement using the same formalism for the intergrowth of the two parent structures^{2,3} (member of the Farey tree hierarchy), with an approximate commensurate modulation $11/18 = 3/5 \oplus 8/13$.

Experimental Section

Synthesis and Analysis. $\text{Zn}_{75.7(7)}\text{Pd}_{24.3}$ and $\text{Zn}_{78.8(7)}\text{Pd}_{21.2}$ were prepared from the elements in the corresponding stoichiometric ratios using Zn pellets (99.999%, Aldrich) and Pd rods (99.9%, Aldrich) placed in sealed, evacuated silica tubes, and heated at 1023 K for 2 days. After naturally cooling to room temperature by turning off the furnace, shiny crystals of the targeted phases were observed. Upon exposure to air and moisture over a one-month period, these crystals remained stable toward noticeable decomposition either visually or by diffraction experiments.

Single crystals, which were studied by X-ray diffraction, were also examined by energy dispersive X-ray spectroscopy (EDXS) performed on a Hitachi S-2460N ESEM. The average chemical formulas determined by EDXS using 15 point measurements gave $\text{Zn}_{75.4(6)}\text{Pd}_{24.6}$ and $\text{Zn}_{78.2(6)}\text{Pd}_{21.8}$, which fell within one standard deviation of the compositions refined by single crystal diffraction, that is, $\text{Zn}_{75.7(7)}\text{Pd}_{24.3}$ and $\text{Zn}_{78.8(7)}\text{Pd}_{21.2}$. Furthermore, each point measurement gave the identical chemical analysis within 0.2 mol percent. To obtain the quantitative values in EDXS, elemental Zn and Pd were used as standards.

X-ray Diffraction (XRD) Data Collection. Owing to the expected quality of the results, special care was paid to the selection of single crystals to be used for structure determinations. Silvery block-shaped crystals were selected and mounted on glass capillaries. Preliminary selection of good quality crystals was first carried out by rapid scans on a Bruker APEX X-ray diffractometer and the two best crystals for each composition were used for subsequent data collections. Both crystals from

the same batch were fully analyzed and gave similar refinement results (atomic positions, site occupancies, etc.). For each crystal, we report the data set that contained the greater number of observed reflections.

Data collection was carried out on a Bruker APEX X-ray diffractometer equipped with monochromated Mo $K\alpha$ radiation ($\lambda = 0.71073 \text{ \AA}$) at ambient temperature, about 293 K. Each data set was consistent with an orthorhombic crystal class and could be described by a *C*-centered Bravais lattice ($a \approx 9.11 \text{ \AA}$ and $b \approx 12.93 \text{ \AA}$ for both samples; $c \approx 33.32 \text{ \AA}$ for $\text{Zn}_{75.7(7)}\text{Pd}_{24.3}$ and $c \approx 46.89 \text{ \AA}$ for $\text{Zn}_{78.8(7)}\text{Pd}_{21.2}$). However, the misfit characters of the structures with two distinct main subsystems and satellite reflections were clearly observed in the diffraction patterns.

XRD Data Processing. Data reduction, absorption corrections, and all refinements were carried out using the *JANA 2006* program package.¹² Measured intensities were corrected for Lorentz and polarization effects. Prior to Gaussian-type analytical absorption corrections, optimizations of the crystal sizes based upon a choice of 364 (Crystal 1) and 385 (Crystal 2) equivalent reflections were performed with the STOE X-shape program.¹³

Prior to data averaging, each Fourier wavevector was indexed with four indices in the M^* vector module of rank 4. Both data sets were averaged according to the (*mmm*, $11\bar{1}$) point group. For $\text{Zn}_{75.7(7)}\text{Pd}_{24.3}$, the same number of independent observed reflections was obtained as the number we found using the classical 3D treatment. Combined with the general condition, the special reflection conditions $h0lm: m = 2n$ and $hk00: h = 2n$ suggested a possible orthorhombic superspace group: *Cmce*-(00γ), which agrees with our previous 3D refinement because the commensurate case for $\gamma = 8/13$ leads to space group *Cmce* for $t = 0$ and equivalent values of the 3D section.

Results

(3 + 1) D Refinement for $\text{Zn}_{75.7(7)}\text{Pd}_{24.3}; q = (8/13)c^*$. As previously mentioned, to develop an accurate (3 + 1)D refinement model of these γ -brass related, Zn-rich Zn–Pd structures, we initially treated $\text{Zn}_{75.7(7)}\text{Pd}_{24.3}$, which possesses a periodicity along the *c*-axis close to 33 Å. From the precise centering of 841 reflections and with (3 + 1)D integer indexing, the refinement of the cell parameters with the SMART software led to the following lattice parameters: $a_s = 12.929(3) \text{ \AA}$, $b_s = 9.112(4) \text{ \AA}$, $c_s = 2.5631(7) \text{ \AA}$, $q = 0.61538(1)c^* \approx (8/13)c^*$ and $V_s = 302.1(3) \text{ \AA}^3$. The structure refinement was initiated based on the information obtained from the classical 3D structure. In the *Cmce*-(00γ) superspace group assigned to $\text{Zn}_{75.7(7)}\text{Pd}_{24.3}$, we determined that four atomic sites in the asymmetric unit assigned to two different subsystems with periodicities of 8 and 13 along the c_s -direction were enough to describe the basic average structure (see Figure 1): the first subsystem consists of one M1 atom at (0, 0, 0); and the second subsystem contains three atoms, M2 at ($\sim 1/8$, $1/4$, $3/4$), M3 at (0, $1/4$, $1/4$), and M4 at ($\sim 1/6$, $\sim 3/5$, $3/4$). On the basis of our knowledge of the cubic γ -brass structure of $\text{Zn}_{81.9(6)}\text{Pd}_{18.1}$,² these M1–M4 sites have been attributed, at first, to fully occupied Zn1, Zn2, Pd3, and Zn4 atoms, respectively. The two subsystem reflection sets are obtained from the (3 + 1)D superspace reflection indices defined by the W^1

(7) Gourdon, O.; Gout, D.; Williams, D. J.; Proffen, T.; Hobbs, S.; Miller, G. J. *Inorg. Chem.* **2007**, *46*, 251.

(8) Morton, A. J. *Electron Microsc., Pap. Int. Congr.*, 9th **1978**, *1*, 342.

(9) Janssen, T.; Looijenga-Vos, A.; de Wolff, P. M. In *International Tables for X-Ray Crystallography, Vol. C: Mathematical, Physical and Chemical Tables*; Wilson, A. J. C., Ed.; Dordrecht: Kluwer Academic Publishers, 1993; Chapter 9.8.

(10) De Wolff, P. M. *Acta Crystallogr.* **1974**, *A30*, 777.

(11) Van Smaalen, S. *Crystallogr. Rev.* **1995**, *4*, 79.

(12) Petricek, V.; Dusek, M.; Palatinus, L. *Jana2006*; The crystallographic computing system. Institute of Physics: Praha, Czech Republic, 2006.

(13) *Stoe X-Shape: Crystal optimization for numerical absorption correction*; Stoe & Cie GmbH: Darmstadt, Germany, 1996.

(14) Van Smaalen, S. *Z. Kristallogr.* **2004**, *219*, 681.

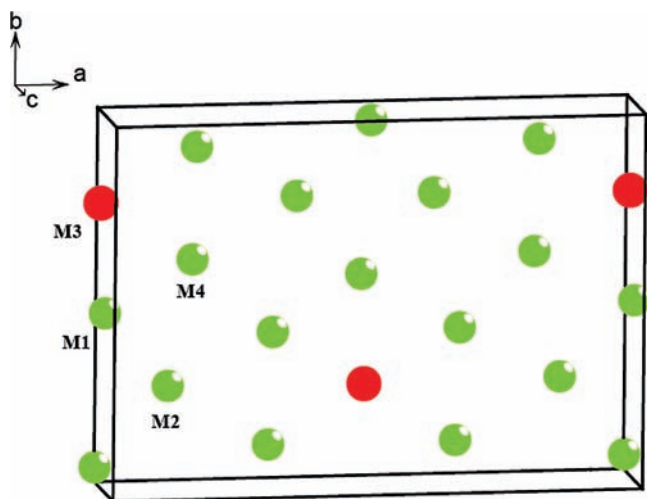


Figure 1. Projection along the c -axis of the average structures of $\text{Zn}_{75.7(7)}\text{Pd}_{24.3}$ and $\text{Zn}_{78.8(7)}\text{Pd}_{21.2}$. Green spheres and red spheres, respectively, represent atomic sites fully or mostly occupied by Zn atoms and Pd atoms.

and W^2 transformation matrices, respectively:

$$W^1 = \begin{pmatrix} 1 & 0 & 0 & 0 \\ 0 & 1 & 0 & 0 \\ 0 & 0 & 1 & 0 \\ 0 & 0 & 0 & 1 \end{pmatrix} \quad \text{and} \quad W^2 = \begin{pmatrix} 1 & 0 & 0 & 0 \\ 0 & 1 & 0 & 0 \\ 0 & 0 & 0 & 1 \\ 0 & 0 & 1 & 0 \end{pmatrix}$$

(for a complete description of the concepts and notations used for incommensurate composite structures, see refs 11 and 14 and references therein). Within one e.s.d., the γ component of the \mathbf{q} wavevector can be considered as rational and equal to $8/13$ ($= 0.615384\dots$). Therefore, the $\text{Zn}_{75.7(7)}\text{Pd}_{24.3}$ structure should a priori be considered as commensurate, an assumption confirmed by subsequent refinement steps. Indeed, the incommensurate approach using the refined irrational value ($= 0.615384\dots$) did not improve the refinement results in any way. For additional information regarding the details of the data collection, see Table 1.

Now, in a composite structure, each subsystem is modulated by the other subsystems, and the refinement of such a structure proceeds as follows: A superspace model of the crystal structure is first developed by refinement of the basic average structure (as in Figure 1) against the main reflections and, thereafter, modified by subsequent introduction of modulation parameters on atomic positions, site occupations, and Debye–Waller factors (DWF). Refinement concludes by fitting against the complete data set including satellite reflections. The modulation parameters are classically written as

$$\mathbf{u}(\bar{x}_4^\nu) = \sum_{n=1}^k s_n \sin(2\pi n \bar{x}_4^\nu) + \sum_{n=1}^k c_n \cos(2\pi n \bar{x}_4^\nu)$$

with s_n and c_n being the refined coefficients of the n th order harmonic. The fourth superspace coordinate is defined as $\bar{x}_4^\nu = t + \mathbf{q} \cdot \bar{\mathbf{x}}^\nu$, with $\bar{\mathbf{x}}^\nu$ being the position of site ν in the basic average structure and t the phase of the modulation. For $\text{Zn}_{75.7(7)}\text{Pd}_{24.3}$, therefore, the residual R -factor smoothly converged to a value of 9.3% upon the addition of successive displacive Fourier amplitude waves.

By analyzing the amplitudes of the modulations and the nature of the individual atomic domains, we may include an additional non-standard centering operation $(0, 1/2, 1/2, 1/2)$, which along with C -centering, doubles the number of symmetry elements even if we keep the same structural description and the supercell space group. Using this additional centering is consistent with the strategy to generalize the refinement of the intergrowth compounds in this γ -brass related, Zn-rich Zn–Pd system, and to find the most symmetrical representation. Therefore, in our final refinements we considered $Xmmm-(00\gamma)0s0$ as the preferred superspace group and we modified the symmetries of components of the modulations to agree with this new symmetry assignment. Notice that this extra centering operation $(0, 1/2, 1/2, 1/2)$ introduces the general reflection condition $k + l + m = \text{even}$ which is satisfied according to the reflection pattern.

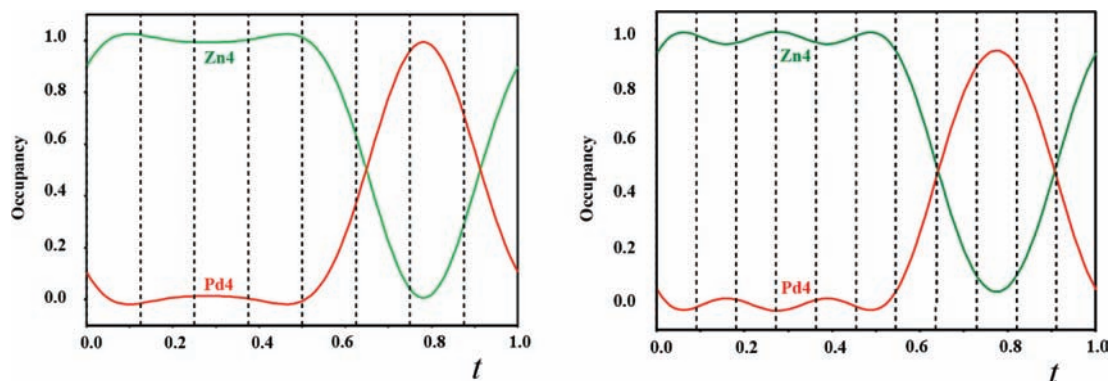
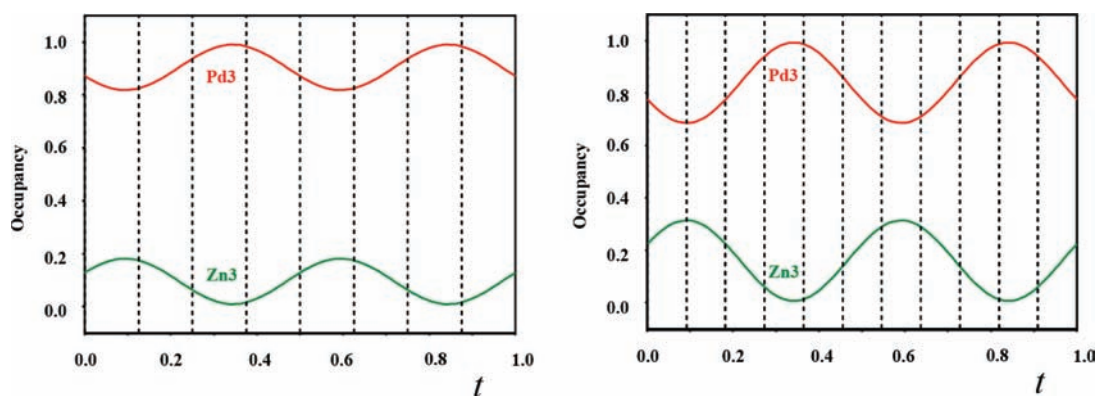
After analyzing the DWF parameters, we observed the possibility of mixed Zn/Pd occupancy on the M4 sites. Therefore, we constrained one Zn4 atom and one Pd4 atom to have the same displacive modulations and to fulfill the site completely via complementary occupation modulations. Each additional modulation wave was checked regarding improvement of the refinement as well as their corresponding physical meaning. By adding displacive Fourier amplitude waves and DWF amplitude waves up to eighth-order for Zn1, to seventh-order for Zn2, Zn4, Pd4, to fifth-order for Pd3, and to third-order for occupancy waves of Zn4/Pd4 sites, the refinement slowly converged to the R value around 5% for 157 parameters. Figure 2 illustrates the occupation modulations for the Zn4/Pd4 sites as a function of the t coordinate.

Occupancy modulations of Zn and Pd atoms on the M4 site are key points of the refinement since the addition of only three parameters drastically improves the R -value from $\sim 9\%$ to $\sim 4\%$. The shapes of these occupancy modulations suggest that the distribution of the Zn4/Pd4 atoms could also be described by using crenel functions.¹⁵ Crenel functions are usually preferred to analyze occupancy modulations for many respects. First, they dramatically reduce the number of refined parameters. Indeed, only two parameters are required to describe an occupation crenel function for an atom ν : the crenel width (Δ^ν) and the crenel midpoint (\hat{x}_4^ν). Second, they avoid non-physical occupation probabilities inherent in the use of a limited number of harmonic functions in the Fourier series expansion. Finally, they prevent intermediate situations produced by the Fourier series expansion at the crenel-like “steps”. Such a procedure was initiated and tested for the occupation modulations at the M4 site in $\text{Zn}_{75.7(7)}\text{Pd}_{24.3}$. Two crenel functions were constructed, one for Zn4 and another one for Pd4, so that these two atoms would be perfectly ordered. According to the chemical composition, we estimated the crenel widths and midpoints to be $\hat{x}_4^{\text{Zn4}} = 0$ and $\Delta^{\text{Zn4}} = 3/4$ for the Zn4 atom, and $\hat{x}_4^{\text{Pd4}} = 1/2$ and $\Delta^{\text{Pd4}} = 1/4$ for the Pd4 atom. These crenel functions slightly improve the refinement by 0.2% for one less parameter, although some DWF terms in the Pd4 domain did not have physically reasonable

(15) Petricek, V.; van der Lee, A.; Evain, M. *Acta Crystallogr.* **1995**, *A51*, 529.

Table 1. Crystal Data and Experimental Details for the Modulated Compounds $\text{Zn}_{75.7(7)}\text{Pd}_{24.3}$ and $\text{Zn}_{78.8(7)}\text{Pd}_{21.2}$

formula (EDXS)	$\text{Zn}_{75.4(6)}\text{Pd}_{24.6}$	$\text{Zn}_{78.2(6)}\text{Pd}_{21.8}$
formula (refined; XRD)	$\text{Zn}_{75.7(7)}\text{Pd}_{24.3}$	$\text{Zn}_{78.8(7)}\text{Pd}_{21.2}$
crystal color		black
molecular weight ($\text{g}\cdot\text{mol}^{-1}$)	197.78	195.51
crystal system		orthorhombic
superspace group	$Xmmm(00\gamma)0s0$ $X = [(1/2, 1/2, 0, 0); (0, 1/2, 1/2, 1/2); (1/2, 0, 1/2, 1/2)]$	
γ ($q_s = \gamma c^*$)	$0.61538(1) = 8/13$	$11/18$
a_s (Å)	12.929(3)	12.909(3)
b_s (Å)	9.112(4)	9.115(3)
c_s (Å)	2.5631(7)	2.6052(6)
V_s (Å ³)	302.1(3)	306.4(2)
Z	4	4
density (calc., $\text{g}\cdot\text{cm}^{-3}$)	4.399	4.237
no. measured/observed refl.	16766/6097	19388/6001
$hklm$ ranges	$-17 < h < 17$ $-12 < k < 12$ $-5 < l < 5$ $-9 < m < 5$	$-17 < h < 17$ $-12 < k < 12$ $-5 < l < 5$ $-12 < m < 5$

**Figure 2.** Pd4 and Zn4 occupancy modulations of $\text{Zn}_{75.7(7)}\text{Pd}_{24.3}$ and $\text{Zn}_{78.8(7)}\text{Pd}_{21.2}$. (see text for additional details). The dashed lines represent the commensurate sections (8-fold or 11-fold periodicities).**Figure 3.** Pd3 and Zn3 occupancy modulations of $\text{Zn}_{75.7(7)}\text{Pd}_{24.3}$ and $\text{Zn}_{78.8(7)}\text{Pd}_{21.2}$. (see text for additional details). The dashed lines represent the commensurate sections (8-fold or 11-fold periodicities).

values, which indicates further Zn/Pd mixing and imperfectly ordered sites as proposed by the crenel functions. Therefore, for final refinements such step functions were not considered. A sophisticated refinement could be imagined by combining crenel functions with a modulation of the fractional occupancy at the Pd4 domain.

As refinement approached the final stages, we observed two major problems: first, the refined chemical composition was not consistent with EDXS measurements; and, second, a systematic analysis of the DWF terms revealed strong variation at the Pd3 sites as function of t . At this stage, therefore, occupancy modulations were introduced up to second-order for the M3 site to allow Zn/Pd

Table 2. Structural Refinement Statistics of $\text{Zn}_{75.7(7)}\text{Pd}_{24.3}$ and $\text{Zn}_{78.8(7)}\text{Pd}_{21.2}$ in $Xmmm(00\gamma)0s0$

	$\text{Zn}_{75.7(7)}\text{Pd}_{24.3}$	$\text{Zn}_{78.8(7)}\text{Pd}_{21.2}$
R overall	3.16	3.14
R_0 main reflections	2.46	1.83
R_1 (1st order satellites)	2.67	2.63
R_2 (2nd order satellites)	4.35	4.55
R_3 (3rd order satellites)	4.75	7.16
R_4 (4th order satellites)	6.88	10.68

mixing using the same restrictions described above for the M4 site; the results of which are illustrated in Figure 3. These additional parameters improve the refinement by

Table 3. Atomic Coordinates, Fourier Amplitudes of the Occupancy and Displacive Modulation Functions, and Equivalent Isotropic Thermal Displacement Parameters $Zn_{75.7(7)}Pd_{24.3}$ and $Zn_{78.8(7)}Pd_{21.2}$ (Zn Occupancies Listed)

	$Zn_{75.7(7)}Pd_{24.3}$ ($q = (8/13)c^*$)					$Zn_{78.8(7)}Pd_{21.2}$ ($q = (11/18)c^*$)				
	occ.*	x	y	z	U_{eq}	occ.*	x	y	z	U_{eq}
Subsystem 1										
Zn1		0	0	0	0.0132(2)		0	0	0	0.0142(2)
s_1			-0.0569(1)					-0.0571(1)		
s_2				0.0346(3)					0.0398(2)	
s_3			-0.0014(1)					-0.0015(1)		
s_4				-0.0094(2)					-0.0063(3)	
s_5			0.0044(1)					0.0055(1)		
s_6				0.0017(3)					0.0044(5)	
s_7			-0.0007(1)					-0.0008(1)		
s_8				0.0018(5)					0.0038(6)	
s_9								0.0006(2)		
Subsystem 2										
Zn2		0.1234(1)	1/4	3/4	0.0135(2)		0.1241(1)	1/4	3/4	0.0153(2)
c_1			0.0505(1)					0.0505(7)		
s_2				-0.0111(1)					-0.0133(1)	
c_2		-0.0069(1)						-0.0086(5)		
c_3			-0.0059(1)					-0.0058(1)		
s_4				0.0019(2)					0.0033(2)	
c_4								-0.0021(1)		
c_5			-0.0011(1)					0.0006(3)		
s_6				-0.0007(4)					-0.0006(5)	
c_6		0.0002(1)						-0.0004(3)		
c_7			-0.0005(2)					0.0007(2)		
s_8									0.0021(4)	
c_8								0.0008(1)		
c_9								-0.0015(2)		
s_{10}									0.0014(4)	
c_{10}								-0.0009(1)		
M3	0.09(2)	0	1/4	1/4	0.0077(1)	0.16(2)	0	1/4	1/4	0.0083(1)
c_1			-0.0250(1)					-0.0242(1)		
s_2				-0.0005(1)					-0.0045(1)	
c_2	$\pm 0.086(6)$					$\pm 0.154(5)$				
c_3			0.0033(1)					0.0051(1)		
s_4				0.0033(2)					0.0048(2)	
c_5			0.0009(1)					-0.0019(5)		
s_6									0.0061(9)	
M4	0.74(1)	0.1797(1)	0.5990(1)	3/4	0.0112(1)	0.75(2)	0.1795(1)	0.5989(2)	3/4	0.0121(1)
s_1				-0.0647(2)					-0.0654(3)	
c_1	$\mp 0.446(3)$	-0.0033(1)	-0.0193(1)			$\mp 0.431(3)$	-0.0033(2)	-0.0187(3)		
s_2				0.0116(2)					0.0138(4)	
c_2	$\mp 0.239(3)$	0.0032(1)	0.0048(1)			$\mp 0.231(3)$	0.0030(2)	0.0051(3)		
s_3				-0.0082(2)					-0.0068(2)	
c_3	$\mp 0.052(3)$	-0.0008(1)	-0.0063(1)			$\mp 0.060(3)$	-0.0016(1)	-0.0072(1)		
s_4				-0.0015(2)					-0.0033(2)	
c_4						$\pm 0.24(4)$	-0.0001(1)	0.0001(1)		
s_5				-0.0010(3)					-0.0002(6)	
c_5		0.0002(1)	0.0005(1)				0.0000(3)	0.0003(4)		
s_6				0.0002(4)					-0.0003(6)	
c_6		0.0003(2)	-0.0002(2)				-0.0028(3)	-0.0013(4)		
s_7				0.0000(4)					0.0020(4)	
c_7		-0.0003(1)	-0.0006(2)				-0.0004(2)	-0.0009(2)		

* Occupancy modulation is defined as $P(\bar{x}_4^v) = P_0^v + \sum_{n=1}^k s_n \sin(2\pi n \bar{x}_4^v) + \sum_{n=1}^k c_n \cos(2\pi n \bar{x}_4^v)$.

lowering the R -factor to its final value of 3.22% for 139 parameters. Simultaneously, the refined chemical composition converged to $Zn_{75.7(7)}Pd_{24.3}$, which is within one standard deviation of the values measured by EDXS. Final structural parameters refined for $Zn_{75.7(7)}Pd_{24.3}$, such as atomic coordinates, Fourier amplitudes of the occupancy, and displacive modulation functions, as well as equivalent isotropic thermal displacements are summarized in Tables 2 and 3.

(3 + 1) D Refinement for $Zn_{78.8(7)}Pd_{21.2}$; $q = (11/18)c^*$. A primary goal of this effort to use superspace groups is to

obtain a refinement model for these γ -brass related, Zn-rich Zn–Pd structures that could not only refine a particular composition, such as for $q = 8/11 c^*$, but to generalize it for the entire family of compounds. Therefore, initially refining $Zn_{78.8(7)}Pd_{21.2}$ using the same basic cell as for $Zn_{75.7(7)}Pd_{24.3}$ in $Xmmm(00\gamma)0s0$ but with $\gamma = 11/18$ resulted in rapid convergence of the residual R -factor to about 4.5%, which significantly validates our model as general for this family of structures. During these first refinement steps, the major differences occurred for the Pd3/Zn3 occupancy modulation functions.

On the basis of the q value, additional modulation functions were warranted in the description. The final refinement has been performed using displacive Fourier and DWF amplitude waves up to the ninth-order for Zn1, 10th-order for Zn2, sixth-order for Pd3/Zn3, and seventh-order for Zn4/Pd4, as well as occupancy waves for Pd3/Zn3 and Zn4/Pd4, respectively, up to second- and fourth-orders. Additional modulations would have been authorized, but their needs were not justified based on the refined s_n and c_n parameters. The final refinement slowly converged to the residual R -factor of 3.16% for 175 parameters. Figures 2 and 3, respectively, also illustrate the occupancy modulations for the Zn4/Pd4 and Pd3/Zn3 sites as a function of the t coordinate. Final refinement parameters for $\text{Zn}_{78.8(7)}\text{Pd}_{21.2}$, such as atomic coordinates, Fourier amplitudes of the occupancy, and displacive modulation functions, and equivalent isotropic thermal displacement parameters are listed in Tables 2 and 3 as well.

This example clearly shows how powerful a (3 + 1)D description could be to treat closely related compounds such as $\text{Zn}_{75.7(7)}\text{Pd}_{24.3}$ and $\text{Zn}_{78.8(7)}\text{Pd}_{21.2}$. Indeed, even if both structures are commensurate and could have been treated by a classical 3D treatment, a (3 + 1)D approach allows us to have a better understanding of the chemical factors associated with the change of the modulation vector. Moreover, a classical 3D refinement for $\text{Zn}_{78.8(7)}\text{Pd}_{21.2}$ would be delicate based on the size of the unit cell as well as the number of parameters to be refined.

Structural Discussion

$\text{Zn}_{75.7(7)}\text{Pd}_{24.3}$ and $\text{Zn}_{78.8(7)}\text{Pd}_{21.2}$ are two members of the family of intergrowth compounds related to the well-known γ -brass structure type. Our recent efforts have already emphasized a 1D description of these intergrowth compounds formed by condensed quasi-infinite chains of Pd-centered clusters along the c -direction.^{2,3} Similar descriptions have been proposed for analogous structures in the Zn–Ni and Zn–Pt systems.^{4,5} Although we will return later to this 1D description, it is interesting to discuss first the additional information obtained from the (3 + 1)D formalism. The Zn/Pd occupancies on two different sites for $\text{Zn}_{75.7(7)}\text{Pd}_{24.3}$ and $\text{Zn}_{78.8(7)}\text{Pd}_{21.2}$, illustrated in Figures 2 and 3, show important information. First, the occupancy modulations of the M4 sites with respect to both Zn and Pd (see Figure 2), sites which form part of the clusters, are quite similar for both structures. The major and essential difference between the two structures, as observed in Figure 3, is the variation of the M3 occupancies for Zn and Pd versus phase t . This result is a significant improvement to the knowledge obtained from the previous 3D studies. Indeed, we were not able to identify any modification to the occupation of the center of these clusters, and assumed that this site was fully occupied by Pd.^{2,3,16} Figure 3 shows clearly that this is not the case, and Figure 4 illustrates how the occupation is modulated from site to site in the two structures. Figure 4 also presents the pseudo-periodicities of the two different substructures, a feature which emphasizes the intergrowth description for these two compounds.

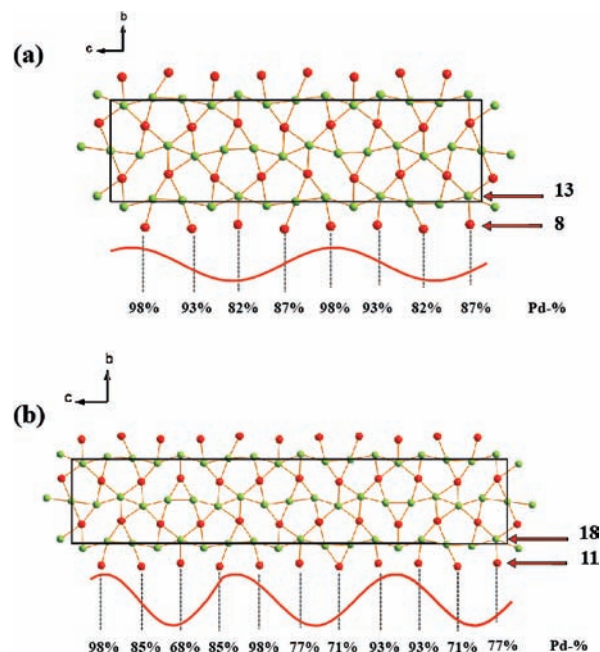


Figure 4. Partial view of the atomic structures of (a) $\text{Zn}_{75.7(7)}\text{Pd}_{24.3}$ and (b) $\text{Zn}_{78.8(7)}\text{Pd}_{21.2}$, showing the pseudo-periodicities of the two different substructures. Below each unit cell is listed the concentration of Pd at the central atom (M3 sites).

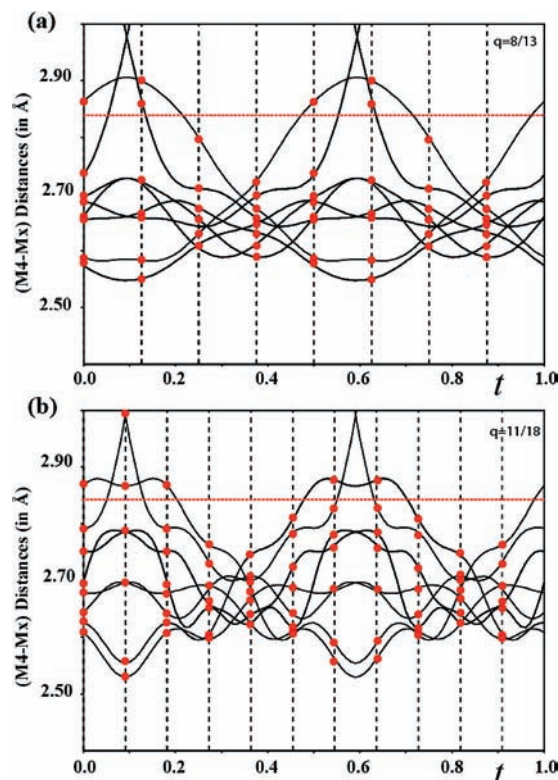


Figure 5. Coordination of (Pd3/Zn3) icosahedra sites by Zn and Pd atoms for (a) $\text{Zn}_{75.7(7)}\text{Pd}_{24.3}$ and (b) $\text{Zn}_{78.8(7)}\text{Pd}_{21.2}$. The black dashed lines represent the commensurate t -sections. The horizontal red dashed line represents the cut off distance chosen for the polyhedron representation (see text for additional details).

This new observation can provide some clues toward understanding the deformations observed from one cluster to another. On the basis of the known crystal structures of the “two parent” phases and using the Farey tree representation,

(16) Pearson, W. B. Z. *Kristallogr.* **1981**, *156*, 281.

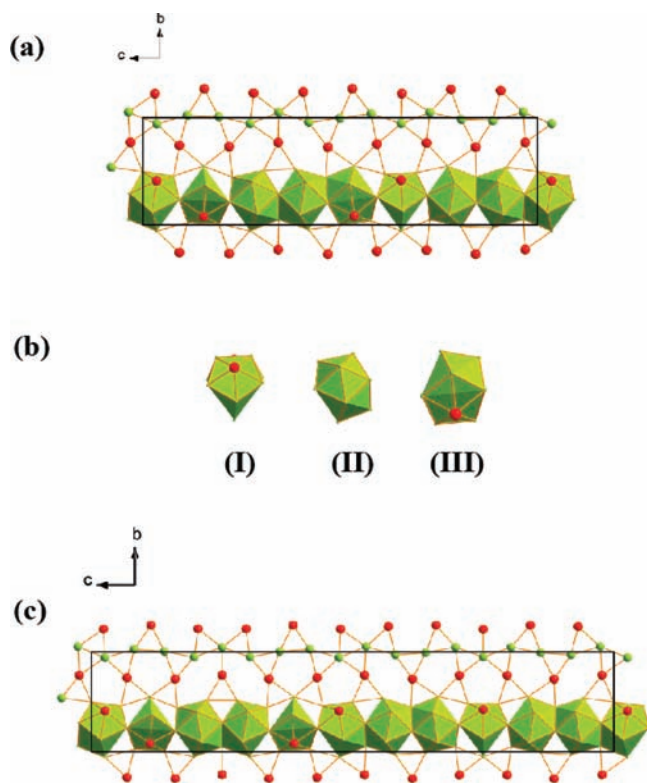


Figure 6. M4-centered clusters connected by either edges or faces in (a) $\text{Zn}_{75.7(7)}\text{Pd}_{24.3}$ and (c) $\text{Zn}_{78.8(7)}\text{Pd}_{21.2}$. Red and green atoms, respectively, represent Pd and Zn. (b) Representation of three major clusters type: (I) Quasi-Icosahedra (QI), (II) nearly regular icosahedra, and (III) distorted icosahedra (see text for additional details).

we hypothesized various intergrowth structures in this family using just two polyhedra: nearly regular icosahedra and quasi-icosahedra.^{2,3} However, the distances within such icosahedra, as illustrated in Figure 5, are not significantly discontinuous, but exhibit a progressive deformation. These “distance versus t ” curves are very powerful tools and an important source of information for many reasons. First of all, there appears to be a direct correlation between the deformation of an icosahedral cluster and the Pd concentration of the central atom. According to Figures 3 and 5, for the t -sections where the M3 site is fully occupied by Pd, the icosahedra are nearly regular, whereas for a Zn-rich situation, the icosahedron is distorted. Moreover, as more Pd is replaced by Zn at the M3 site, the more distorted is the polyhedron.

These distance variations, as illustrated in Figure 5, raise the question of how to select a specific cutoff distance to perform a cluster description for these structures. The red dashed line at 2.83 Å in Figure 5 corresponds to the choice made for our earlier description.^{2,3} It is a subjective choice based on the variations observed in Figure 5 (between “shorter” and “longer” distances), and we agree that other suitable descriptions could be formulated. However, this specific cutoff distance choice is useful because we can still describe our compounds in terms of successions of dimers (DI) and/or trimers (TI) of icosahedra separated by quasi-icosahedra (QI) (see Figure 6). As compared to our previous description,^{2,3} we observe a new polyhedron (see Figure 6b (III)), which is so distorted that it can no longer be considered as an icosahedron (as in II), but is not as distorted as the QI block (I). This block (III) is located close to QI sites and

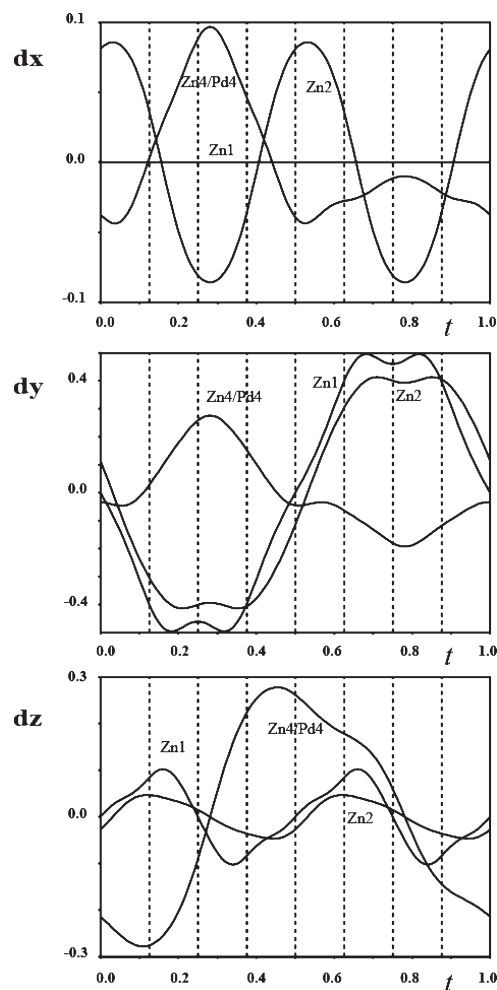


Figure 7. Displacement along the x -, y -, and z -directions vs t for the 12 atoms surrounding the central M3 atoms in $\text{Zn}_{75.7(7)}\text{Pd}_{24.3}$. The black dashed lines represent the commensurate sections.

constitutes part of the TI units, making a cluster succession (II)-(II)-(III) by sharing faces. This block (III) can be described as a 10-vertex polyhedron with two additional atoms at longer distances (ca. 2.88 Å) from the center, atoms which cap two pentagonal faces. As already observed, the DI and TI entities made of face-sharing clusters, are connected by edges to QI clusters (see Figure 6 panels a and c).

To analyze the cluster deformations more closely we examine the dx , dy and dz displacements of the 12 atoms (4 Zn1 atoms, 4 Zn2 atoms, 2 Zn3 atoms, and 2 Zn4/Pd4 atoms) surrounding the central M3 atom as a function of t in $\text{Zn}_{75.7(7)}\text{Pd}_{24.3}$ (see Figure 7). The greater displacements are along the y - and z -directions. Furthermore, displacement of the Zn4/Pd4 mixed site is more significant along the z -direction and less pronounced in the Pd-rich region, when t varies from about 0.6 to 0.9.

If we examine closely the occupation of the 12 atoms surrounding each M3 site, there is an interesting “charge balance” effect. Indeed, when the central atom (M3) is Pd-rich (98%) the polyhedral surroundings is Pd-poor (0.2 Pd for 11.8 Zn); it is opposite for a M3 Pd-poor site (82%, for example), where the surroundings is completed by 1.98 Pd and 10.2 Zn.

This (3 + 1) D description seems a better way as compared to the algorithmic Farey tree to describe and to eventually

predict the atomic structures of other members in this family of intergrowth compounds. Surprisingly, Figure 5 shows that the M4–Mx distances do not depend of the nature of the member that you are looking at. Indeed, both Figures 5a and 5b show distances curves relatively similar. This fact suggests that we could use the Figure 5b (obtained by the refinement of the $q = 11/18$ compound) to predict the cluster description of the $q = 8/11$ compound. Then, we can assume that, to a first approximation, the cluster description given by Figures 5a and 5b is valid for the whole range of compositions. In the limiting case $q = 3/5$, corresponding to the “real” γ -brass, the relevant t values of the section are $t = 0, 1/3, 2/3$. Notice that the $t = 1/3$ values give the most regular icosahedrons, its center being a fully Pd3 site, according to Figure 3.

Summary

The (3 + 1)D superspace approach allowed us to refine unambiguously the atomic arrangement (position and occupation) of two members ($\text{Zn}_{75.7(7)}\text{Pd}_{24.3}$ and $\text{Zn}_{78.8(7)}\text{Pd}_{21.2}$) of intergrowth structures in this Zn-rich region of the Zn–Pd system. Our refinements emphasize a unique Pd/Zn occupation modulation at the center of the icosahedra related to the distortion of the icosahedral sites. This family

of intergrowth compounds is a good example of how powerful the superspace group approach could be since the complexity of this distortion associated with the modulated wave will not have been revealed using a classic 3D treatment.

Acknowledgment. The authors are grateful to Dr. Warren Straszheim at Iowa State University for the EDXS measurements. This work was carried out at the Ames Laboratory, which is operated for the U.S. Department of Energy by Iowa State University under Contract No. DE-AC02-07CH11358. This work was supported by the Materials Sciences Division of the Office of Basic Energy Sciences of the U.S. Department of Energy and the MEC-Spain. Development of the program Jana2006 was supported Praemium Academiae of Czech Academy of Sciences. The authors also wish to thank the reviewers for their thorough review and useful suggestions.

Supporting Information Available: X-ray crystallographic files in CIF format of $\text{Zn}_{75.7(7)}\text{Pd}_{24.3}$ and $\text{Zn}_{78.8(7)}\text{Pd}_{21.2}$ using the (3 + 1)D formalism as well as the projected 3D result. This material is available free of charge via the Internet at <http://pubs.acs.org>.